PERGAMON

Journal of Structural Geology 24 (2002) 1729–1739

JOURNAL OF STRUCTURAL GEOLOGY

www.elsevier.com/locate/jstrugeo

Experimental insights on the geometry and kinematics of fold-and-thrust belts above weak, viscous evaporitic décollement

E. Costa[a,*], B.C. Vendeville[b]

[a]*Dipartimento di Scienze della Terra, Università di Parma, Parco Area delle Scienze, 157/A, 43100 Parma, Italy*
[b]*Bureau of Economic Geology, The University of Texas at Austin, University Station, Box X, Austin, TX 78713, USA*

Received 13 December 2000; revised 22 May 2001; accepted 29 November 2001

Abstract

This paper discusses the differences in mechanical properties and kinematics between fold-and-thrust belts detaching on evaporitic décollements and those detaching on stronger detachments. Physical experiments are described that model shortening of a thick brittle cover overlying a weak, viscous décollement to gain a better understanding of these differences. We tested the influence of (1) the décollement layer thickness and (2) the presence of a deformable backstop on the hinterland side and of a décollement pinch-out on the foreland side. Because of the very low shear strength of the viscous décollement, folds and thrusts did not propagate according to a piggy-back sequence but by centripetal, back-and-forth propagation. Additional shortening was accommodated by growth of all existing structures. Fold symmetry and thrust vergence varied between experiments. Models confined between two rigid, vertical endwalls always deformed by symmetric folding and thrusting. In models having a deformable backstop and a foreland décollement pinch-out, forethrusting initially dominated, folds were asymmetric, and fault blocks rotated. In models having a thick décollement layer, folds kept growing asymmetrically. Diapirism also depended on the initial décollement geometry. Diapirs formed only in models having a deformable backstop and were restricted to the hanging wall of a fault-related fold. Finally, the implications of such kinematics on the thermal history are discussed as well as the likelihood of hydrocarbon maturation and preservation.

Keywords: Physical models; Salt tectonics; Fold-and-thrust belts; Kinematics; Geometry; Diapirism

1. Introduction

Fold-and-thrust belts detaching on non-evaporitic horizons (e.g. overpressured shale) have been the topic of numerous research projects and published articles (e.g. Davis et al., 1983; Suppe, 1983; Dahlen et al., 1984; Price and Fermor, 1985), and their general geometric and kinematic characteristics are reasonably well understood. Most such belts form a wedge whose topographic surface dips toward the foreland by a few degrees (3–5°) (Dahlen et al., 1984). The belt grows and advances by maintaining a self-similar geometry. As the wedge lengthens by forward propagation of its front, it also thickens to maintain this critical taper, whose value is controlled by the angle of internal friction and the cohesion of the cover rocks and the coefficient of friction along the detachment horizon (Dahlen et al., 1984). Although variations do occur between different foldbelts, the general trend is that foldbelts advance toward the foreland by nucleation of younger structures at or in front of the toe of the wedge, whereas older structures within the wedge continue to grow or rotate passively—albeit more slowly—in order to accommodate the thickening required to maintain a constant wedge taper.

By contrast, fold-and-thrust belts that detach along low-viscosity evaporitic décollement layers have been less extensively studied, and their geometry and kinematic histories markedly differ from those of fold-and-thrust belts having higher basal friction. Examples of evaporitic detachment include some thin-skinned, but tectonically driven foldbelts, such as the Jura (Laubscher, 1977; Philippe et al., 1996), the central Appalachian (Davis and Engelder, 1985, 1987), the Appennines (Coward et al., 1999), the Romanian Carpathian (Stephanescu et al., 2000), the Salt Range in Pakistan (Butler et al., 1987; Davis and Lillie, 1994; Cotton and Koyi, 2000), the Sierra Madre Oriental in northeast Mexico (Camerlo, 1998; Fischer and Jackson, 1999; Marrett, 1999), and the Mediterranean ridge offshore Libya (Von Huene, 1997; Mascle et al., 1999). Examples also include gravity-driven foldbelts along salt-bearing continental margins offshore the U.S. Gulf Coast (Perdido

* Corresponding author. Fax: +39-0521-905-305.
E-mail addresses: costae@ipruniv.cce.unipr.it (E. Costa), bvdv@mail.utexas.edu (B.C. Vendeville).

0191-8141/02/$ - see front matter
PII: S0191-8141(01)00169-9

and Mississippi-fan foldbelts; Wu, 1993; Peel et al., 1995; Rowan, 1997; Fiduk et al., 1999; Trudgill et al., 1999), Angola and Brazil (Spencer et al., 1998; Marton et al., 2000), northern Egypt (Sage and Letouzey, 1990; Gaullier et al., 2000), and in the western Mediterranean (Golfe du Lion; Bellaiche, 1993; Valette and Benedicto, 1995).

Commonly, the geometrical characteristics of foldbelts detaching on salt are that structural vergence of folds or thrusts is more symmetrical (both forward and backward) whether the detached cover deforms by folding, where the lithology of the cover makes bedding-parallel slip possible (e.g. the Sierra Madre Oriental in NE Mexico; Marrett, 1999), by faulting where the cover is made of more competent rocks (e.g. the Jura; Philippe et al., 1996), or by a combination of both (Rowan, 1997; Trudgill et al., 1999). All such foldbelts exhibit a very low taper of 1° or less (Davis and Engelder, 1987).

In onshore foldbelts, the precise timing of formation of individual structures during ongoing regional shortening may be difficult to estimate because the syntectonic sediments recording folding and thrusting have typically been eroded away. Moreover, because the low taper of foldbelts above salt allows them to advance and propagate much faster than those detaching on stronger décollements, the time interval between the formation of different folds or thrusts within a given belt may well be too short to be clearly recorded by syntectonic sediments or to be resolved at the scale of standard chronostratigraphy. Finally, several studies have documented break-back thrusts that formed behind older thrusts (Eastern Spanish Pyrenees foreland; Puigdefàbregas et al., 1992), or have indicated that many structures within a foldbelt can grow simultaneously (Boyer, 1992).

Gravity-driven foldbelts above salt, which are typically located offshore, provide a syntectonic record of fold propagation. For example, folds in the Mississippi-fan foldbelt (deep-water US Gulf of Mexico) formed and grew coevally (Wu, 1993; Rowan, 1997). In the Perdido foldbelt (deep-water US Gulf of Mexico; Trudgill et al., 1999), folds first formed coevally, but the most external (i.e. downdip) folds stopped growing, whereas folds located landward were later reactivated (Rowan, 1997; Trudgill et al., 1999). Unfortunately, it is likely that the kinematic evolution observed in gravity-driven foldbelts cannot be confidently extrapolated to tectonically driven foldbelts because their origins differ. Formation and growth of gravity-driven foldbelts is controlled by gliding and spreading of the sediments along the slope of the continental margin. Both processes are controlled by the angle of the margin slope, itself dependent on thermal and tectonic subsidence of the basin margin, and on rates of sediment progradation and aggradation. Moreover, the amount of finite shortening in gravity-driven fold-and-thrust belts is much lower than that in their tectonically driven counterparts (Rowan, 1997; Trudgill et al., 1999; Rowan et al., in press). Unlike in tectonically driven foldbelts, where shortening progresses toward the foreland, shortening in gravity-driven foldbelts above salt typically occurs in the external zones, near the tip of the sediment wedge or near the seaward salt pinch out, and sometimes progresses updip, where the wedge of brittle sediments is thicker (Rowan et al., in press).

Because of these complications, we chose an experimental approach to investigate the kinematics of fold-and-thrust propagation during tectonically driven shortening. Experimental modeling had the advantages of providing 4-D information (including the evolution through time) and of allowing us to systematically vary some of the system's parameters. Our study completes the previous experimental works by Cobbold et al. (1989), McClay (1989), Dixon and Liu (1992), Liu Huiqi et al. (1992), Letouzey et al. (1995), Koyi (1998), and Cotton and Koyi (2000). Our goal was to conduct experiments whose design included two key parameters of wide fold-and-thrust belts above evaporites. First, few previous models (except for Cotton and Koyi, 2000) have taken into account the extremely low strength of a viscous, evaporitic décollement when deformed under typical tectonic displacement rates (i.e. a few cm/year or less). Second, we wanted to construct models that were as 2-D as possible to be able to later discriminate between the relative contributions of 2-D and 3-D parameters, such as lateral edge effects, onto the development of thrust belts. For example, experiments by Vendeville (1991) have demonstrated that, where the basal décollement is weak, fold-and-thrust belts are very sensitive to lateral friction. Changing the amount or sense of shear along the model's sidewalls can change the wedge taper and even reverse the sense of thrust-and-fold propagation. Most previously published models had either a basal décollement that was too strong to properly simulate a layer of weak, viscous evaporites, and/or had significant friction between the mobile part of the cover, underlain by the décollement, and its lateral sides. For example, in Cotton and Koyi (2000), one half of the model was underlain by a weak viscous layer, whereas the other half rested on a stronger, frictional detachment. Such setup imposed friction between the more mobile and less mobile parts of the model. The experiments we present in this article suggest that the pattern of forward fold-and-thrust propagation observed in Cotton and Koyi's experiments does not occur in plain-stress, plain-strain models, where the influence of lateral friction has been reduced by lubricating the model's lateral boundaries.

The design of the experimental protocol and choice of parameters used in our modeling work were driven by a preliminary analysis of the dynamic properties proper to fold-and-thrust belts detaching on salt. We first present the conclusions of this analysis, then illustrate the design and results of the physical experiments. We also discuss the influence of the initial system geometry on the development of salt diapirs and discuss a few implications of model results in terms of hydrocarbon potential of fold-and-thrust belts.

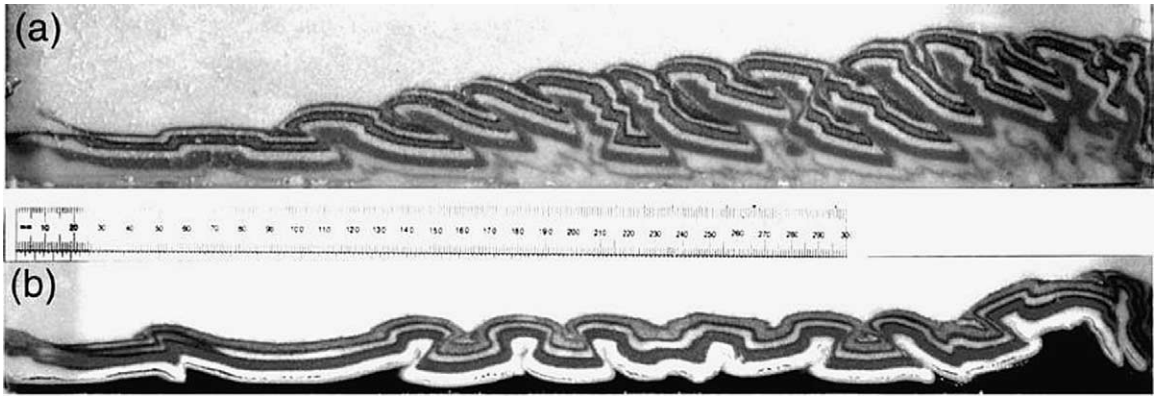

Fig. 1. Two cross-sections with contrasting décollement layers. In both models, shortening was applied by moving a vertical rigid wall (right-hand side) leftward. (a) Model comprising a brittle cover (dry sand) overlying a strong, frictional décollement (glass microbeads: two lowermost white layers in photograph). Deformation was preferentially accommodated by slip along forethrusts that propagated leftward in piggy-back fashion. (b) Model comprising a brittle sand cover resting above a weak, viscous décollement (silicone polymer; black basal layer in photograph) and deformed at low strain rate. Folds were symmetrical and grew coevally.

2. Mechanical and dynamic properties of fold-and-thrust belts detaching on salt

The basal shear stress resisting the advance of a foldbelt above a frictional material (e.g. shale) depends on the thickness and density of the sediment cover, the amount of frictional resistance along the detachment plane, and the coefficient of fluid pressure along that detachment. In the case of an ideal frictional-plastic behavior (i.e. Mohr–Coulomb) for the rocks forming the detachment, the shear stress resisting translation of the overlying cover depends on the lithostatic stress but is independent of the strain rate. Assuming a uniform cover thickness, h, of 3000 m, a density, ρ, of 2500 kg m^{-3}, a coefficient of friction along the detachment, f, of about 0.6 (Hubbert and Rubey, 1959; Byerlee, 1978; Weijermars et al., 1993), and a coefficient of fluid pressure, λ, of 0.8, the shear stress, τ, required to cause slip at the base of a brittle cover would be:

$$\rho g h f(1 - \lambda) = 8.83 \text{ MPa} \quad (1)$$

Fig. 1a illustrates the geometry of a model detaching on a frictional substratum. Because of the relatively high basal friction, the foldbelt defined a foreland-dipping wedge that advanced by forming new thrust-bounded folds at its front while older thrusts were less active and merely accommodated the thickening of the wedge. Younger thrusts carried older thrusts in their hanging wall in a piggy-back fashion. Basal friction also favored preferential slip along forethrusts. Backthrusts ceased to move soon after their initial formation.

By contrast, the estimated strength of a low-viscosity décollement is at least one order of magnitude lower. In contrast to shale detachments, resistance to translation of the overlying brittle cover does not take place by slip along one or several fault planes but is accommodated by simple shear (i.e. Couette flow) of the entire thickness of the viscous décollement layer (Kehle, 1970; Weijermars et al., 1993). The viscous shear stress resisting deformation is independent of the thickness of the brittle cover, but depends on the thickness of the viscous layer and the shear-strain rate (Weijermars et al., 1993). For example, assuming an evaporitic décollement layer having a thickness, h, of 1000 m, a constant viscosity, η, of 1×10^{18} Pa s, and subjected to a constant linear displacement rate, v, of about 1 cm year^{-1}, the resulting basal shear stress in the viscous layer, τ, would be:

$$\tau = (v/h)\eta = 0.32 \text{ MPa} \quad (2)$$

a value 27 times lower than that in Eq. (1) for shear strength of a shale detachment having a coefficient of fluid pressure, λ, of 0.8. This value also illustrates that tectonic stresses within the salt layer are much lower than those in the overlying brittle section. For example, assuming a brittle cover made of 3000 m of sediments and having a volumetric mass, ρ, of 2500 kg m^{-3}, a coefficient of friction of 0.6, and negligible cohesion, the differential stress for compression would be close to 147.15 MPa. The value for basal shear stress would further decrease if the salt layer was thicker or if salt viscosity was reduced by temperature increase, by strain softening due to crystal-size reduction, or by an increase in fluid content.

The principal result of such low basal shear resistance is that the associated critical wedge taper should be extremely low (Fig. 1b and Davis and Engelder, 1987). Therefore, even for minor amounts of shortening and displacements of the backstop, a foldbelt detaching on salt would rapidly advance and lengthen, as its tip would rapidly propagate forward, but the foldbelt should experience only minor thickening. Theoretically, such minor shortening could take place by formation of (1) numerous, closely-spaced folds or thrusts that subsequently do not grow, or (2) fewer, widely-spaced structures that undergo significant growth. Experiments suggest that the latter pattern prevails

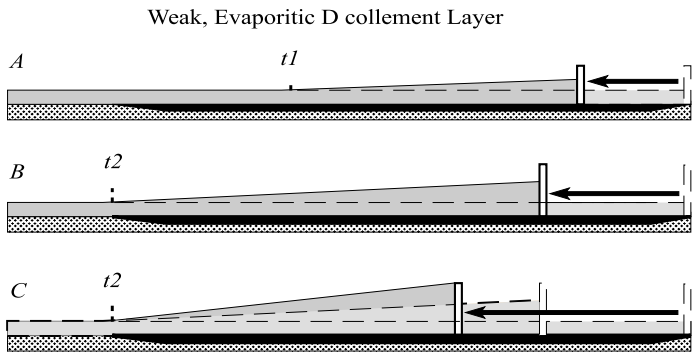

Fig. 2. Cartoon illustrating the evolution of a contractional wedge (gray) above a weak, viscous décollement (black). The wedge first advances forward while retaining a self-similar geometry (A to B), then its front reaches the foreland pinch-out of the décollement (B). Subsequent deformation must be accommodated by horizontal shortening and vertical thickening of the whole wedge (C).

during the early deformation history of fold-and-thrust belts (Fig. 1b).

Because the front of the fold belt advances rapidly, it can theoretically reach the foreland pinch-out of the salt décollement early (Fig. 2), when the amount of regional shortening is still small and the belt comprises only a few, widely-spaced folds and thrusts. Once the foldbelt front has reached the salt pinch-out, it can no longer obey the condition of geometric self-similar growth, according to which the wedge's length and height increase proportionally so that the wedge taper remains constant. Instead, additional shortening must be solely accommodated by coeval horizontal shortening and vertical thickening in a manner similar to that of a stiff layer (the brittle cover) resting on a low-viscosity matrix (the salt) as described by Biot (1961) and Ramsay (1967). From a kinematic perspective, this phase of shortening can be accommodated by (1) formation of new folds and thrusts within the belt, (2) continued growth of old folds and thrusts, or (3) a combination of both. The experiments below were designed to better understand how this change in foldbelt kinematics takes place.

3. Experimental setup and scaling

3.1. Scaling

The primary goal of our experiments was to apply a lot of shortening to models of large fold-and-thrust belts above salt. Therefore, the models were initially long (between 96 and 127 cm) and the backstop moved between 29.8 and 46 cm (31–36% of finite shortening). The shortening continued at a constant rate for different durations (61–99 h). The models comprised an isotropic layer of dry quartz sand (3.0 cm thick), representing a brittle sediment cover, overlying a layer of Newtonian viscous, transparent silicone polymer (EL Polymer NA, a polydimethyl siloxane manufactured by Wacker Silicones, USA), representing a layer of viscous rock salt. Dry quartz sand has been used extensively in physical modeling. Sand obeys a Mohr–Coulomb criterion of failure, has an angle of friction of about 30° and a low cohesion, which makes it an excellent analog material for brittle rocks in the upper continental crust (Krantz, 1991; Schellart, 2000). The viscous silicone polymer used has rheological properties similar to those of various other polymers used in previous modeling of salt systems. Within the range of strain rates used in this study (lower than $10^{-2}\,s^{-1}$), the silicone polymer, like rock salt, behaves as a Newtonian fluid and has a very low yield strength.

From a scaling perspective, the model-to-prototype ratio for lengths, L^*, was 1×10^{-5} (1 cm in experiments represented 1000 m in nature). Hence, models simulated a 500–1000-m-thick salt layer overlain by a 3000-m-thick brittle cover, about 100 km long. Following the rules of scaling analysis described by Hubbert (1937), Ramberg (1967), Vendeville et al. (1987), and Eisenstadt et al. (1995), the model-to-prototype ratio for stresses, σ^*, must be as follows:

$$\sigma^* = \rho^* g^* L^* \tag{3}$$

where ρ^* is the scaling ratio for densities and g^* is the ratio for the gravity acceleration. Because our models were deformed in a natural gravity field, the ratio for gravity acceleration, g^*, was one. The material density of the model materials was about half that of natural rocks, hence the density ratio, ρ^*, was 0.5. This made the stress ratio, σ^*, be 5×10^{-6}. The viscosity ratio between model and natural prototype, η^*, was between 1×10^{-13} and 1×10^{-14}, assuming a viscosity for salt rock varying between 1×10^{17} and 1×10^{18} Pa s^{-1} and a viscosity of 1×10^{4} Pa s^{-1} for the silicone polymer. Therefore, the scaling ratio for strain rate between experiment and nature, ϵ^*, was:

$$\epsilon^* = \sigma^*/\eta^* = 5\times10^{8} \tag{4}$$

(the models deformed 500 million times faster than nature), assuming a salt viscosity value of 1×10^{18} Pa s^{-1}. The value of the strain-rate ratio was 5×10^{7} (the models deformed 50

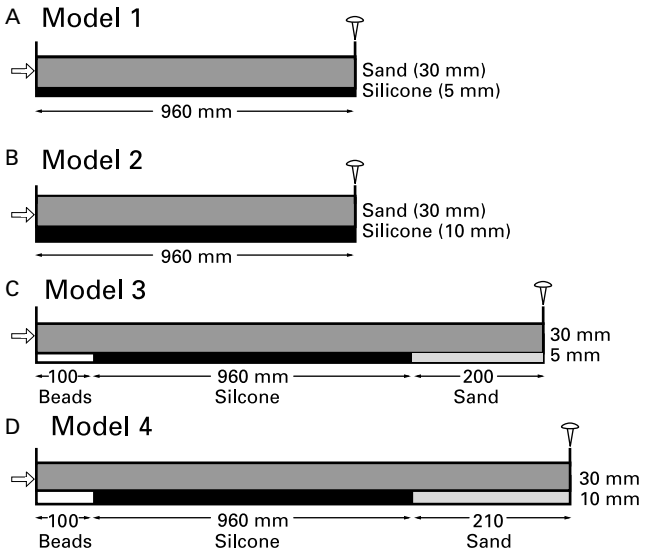

Fig. 3. Line drawing illustrating the initial cross-sectional geometry of the four models discussed in this article. In Models 1 and 2 (A and B), the décollement layer (black) and the sand (patterned) covered the entire model length and abutted against rigid endwalls (both fixed and moving). In all experiments, shortening was applied by moving the left-hand wall right. In Models 3 and 4 (C and D), the décollement layer ended before the moving endwall (left-hand side). There, the sand cover was underlain by a décollement made of glass microbeads and acted as a deformable backstop. In addition, the décollement layer also ended before the fixed endwall (right-hand side), where it was replaced by a layer of dry sand, representing an area having no potential décollement.

million times faster than nature), assuming the lower value for the salt viscosity (1×10^{17} Pa s^{-1}).

The time ratio, t^*, is the inverse of the strain-rate ratio and was 2×10^{-9}, assuming the higher salt viscosity (1×10^{18} Pa s^{-1}); consequently 1 h in experiments represented 57,000 years in nature. Assuming the lower salt viscosity (1×10^{17} Pa s^{-1}), $t^* = 2 \times 10^{-8}$ and 1 h in experiments represented 5700 years in nature. Therefore, our experiments, which ran for 61–99 h, represented a range of geological time of 3.5–5.6 Ma (assuming a high salt viscosity), or 348,000–564,000 years (assuming a low salt viscosity).

The models were deformed by moving one endwall at a rate of 0.5 cm h^{-1}. The ratio, v^*, for velocities between model and nature is the product between the length ratio, L^*, and the strain-rate ratio, ϵ^*. Therefore, assuming a high salt viscosity (1×10^{18} Pa s^{-1}), our experiments simulated shortening occurring in nature at a velocity of 1 cm year^{-1}. Assuming a low salt viscosity (1×10^{17} Pa s^{-1}), the equivalent shortening velocity in nature was about 10 cm year^{-1}.

3.2. Initial setup

Fig. 3 illustrates the initial cross-sectional geometry used in the four experiments presented in this article. All models had an initially tabular basal viscous layer (0.5 or 1 cm thick) overlain by a 3-cm-thick tabular brittle cover made of several sand layers having different colors but identical mechanical properties. There was no mechanical anisotropy within the brittle cover.

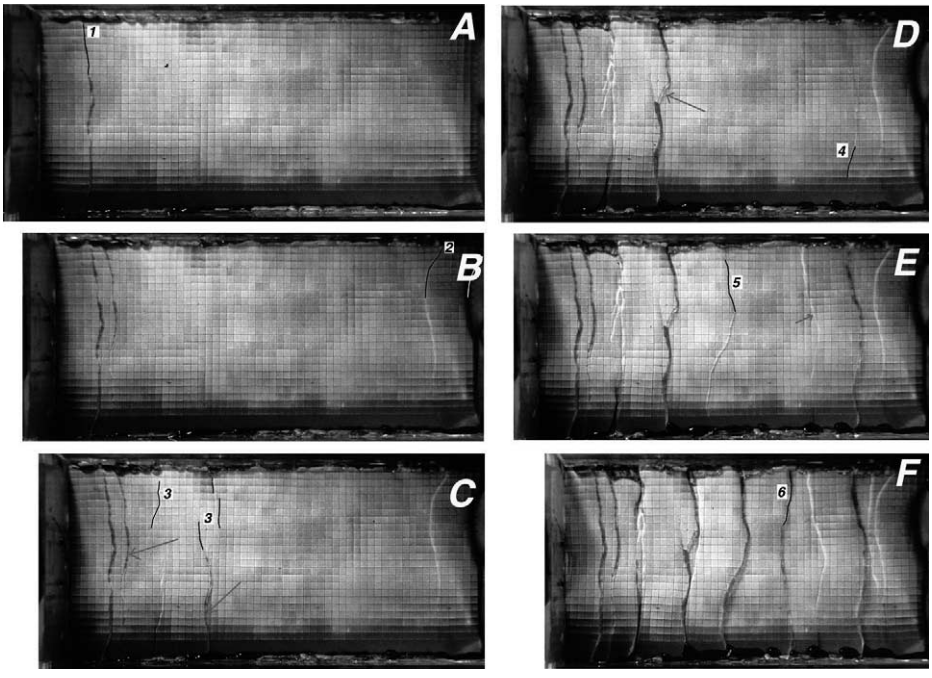

Fig. 4. Overhead photographs of Model 1 during deformation. Each photograph was shot immediately after a new box fold formed. Black lines outline the traces of thrust plane(s) or kink band(s) bounding each new box fold. The photos indicate that deformation started with one or two box folds located near the backstop (A). Next, a younger fold formed near the frontal pinch-out of the décollement layer (B). Subsequently, younger folds formed between older structures, progressively closer to the center of the model, following an overall centripetal propagation pattern (C–F).

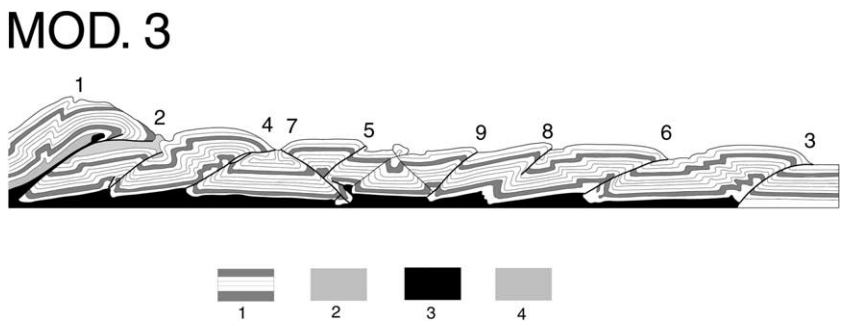

Fig. 5. Line drawing of a vertical cross-section in Model 3 after deformation showing: (1) a fault-related fold, in which the décollement material was incorporated and passively carried as part of the hanging-wall sequence; (2) a triangle zone; (3) superposition of an anticline on top of a syncline. The latter geometry is due to the intersection of two conjugate kink planes within the sand cover: (1) brittle sand cover; (2) glass microbeads (frictional décollement); (3) silicone polymer (weak, viscous décollement); (4) slumped sand.

We tested two different setups. In the first setup (Fig. 3A and B), the viscous décollement layer initially extended across the entire model width and terminated against the rigid, moving endwall, which acted as a vertical, rigid backstop. In the second setup (Fig. 3C and D), the viscous décollement layer did not extend all the way to the endwalls; instead, it ended about 10 cm from the moving endwall. The space between the endwall and the décollement was filled with glass microbeads, a frictional material weaker than sand but significantly stronger than the viscous silicone polymer. This 10-cm-long strip (left-hand side in Fig. 3C and D), acted as a deformable backstop that transmitted the tectonic push from the moving wall but could also fold, fault, or rotate during shortening. On the other side (right-hand side in Fig. 3C and D) of the model, the source layer also ended a few centimeters from the fixed wall, but there the sand layer rested directly on top of the model base and did not deform.

Unlike in previously published experiments (e.g. Cotton and Koyi, 2000), we drastically reduced the influence of lateral friction by lubricating the sand layer from each sidewall using thin vertical coatings of viscous silicone. Because of the low applied strain rate, the silicone coatings offered little or no resistance to forward translation of the model during shortening. This means that little or no lateral shear stresses would interfere with model evolution, thus leading to formation of cylindrical structures and plane-strain deformation. In nature, such conditions would occur in wide and long foldbelts, such as the central Appalachians.

4. Experimental results

Our models provide insights on three aspects of fold-and-thrust belts: (1) the kinematics and mode of propagation of the folds and thrusts, (2) the symmetry of each structure, and (3) the presence or absence of diapirs that formed during shortening.

4.1. Kinematics

In all the experiments, a strong brittle cover was shortened above a very weak décollement layer. The associated shear strength of the décollement layer was low; hence the critical taper required for the deformation zone to advance and propagate forward was very low. The typical progression of deformation in our models is illustrated by a series of overhead photographs shot during deformation (Fig. 4) and by line drawings and photographs of vertical sections cut at the end of the experiments (Figs. 5–8). Fold and fault propagation was recorded by time-lapse overhead photographs and by videotaping. The use of low-angle oblique lighting allowed monitoring of the along-dip propagation of faults and folds because of the shadows cast by the fault scarps. Along-strike fault

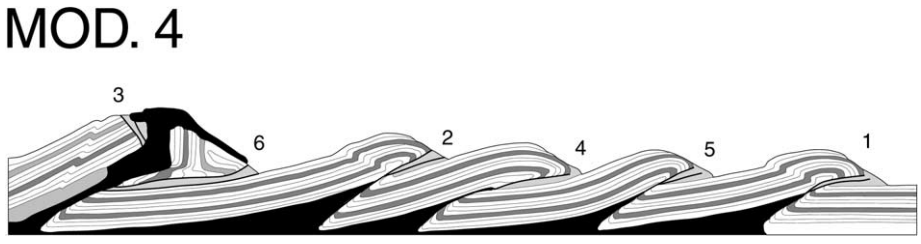

Fig. 6. Line drawing of a vertical cross-section cut in Model 4 (décollement layer twice as thick as that in Model 3). Note the diapir piercing the fault-propagation fold on the right and the normal faults responsible for the thinning of the fold's hinge, which allowed the viscous silicone to rise and emerge. Symbols as in Fig. 5.

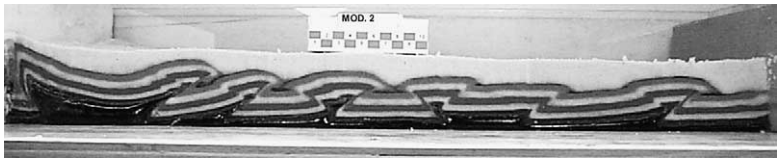

Fig. 7. Photograph of a cross-section in Model 2 (thick décollement, no deformable backstop and no décollement pinch-out). Shortening was accommodated by symmetrical box folds. Note the absence of diapirs.

and fold propagation, however, was too fast to be recorded. By the time a fold had grown tall enough to be visible, it had already propagated across the entire model's width.

Deformation started with one or two box folds located near the backstop (Fig. 4A). In all experiments, the box folds were bounded by steep (i.e. 45°) shear zones or kink bands along which reverse movement took place. Next, a younger fold formed near the frontal pinch-out of the décollement layer (Fig. 4B), which indicates that, by that time, the length of the critical wedge had already reached or even exceeded the entire width of the salt basin.

Additional regional shortening could no longer be accommodated by forward advance of the deformation front because there was no potential detachment plane beyond the pinch-out of the viscous décollement. Further advance of the wedge's tip beyond the décollement pinch-out would have required a much steeper wedge taper. Consequently, shortening was accommodated by formation of new thrusts and folds deforming the wedge itself (i.e. the part of the cover overlying the viscous décollement), which thickened but no longer advanced.

Younger folds and thrusts formed between older structures, nucleating progressively closer to the center of the model, and following an overall centripetal pattern of propagation (Fig. 4C–F). The location of these new structures alternated back and forth between the hinterland and the foreland regions of the model.

This particular pattern of formation and growth of new folds and thrusts followed by their replacement by younger ones can be explained in simple mechanical terms. As each individual fault-bounded fold formed, strain softening in the shear zones or kink bands bounding it made the brittle section there weaker than the undeformed surrounding blocks. Therefore, additional regional shortening was preferentially accommodated by growth of this fold. However folds in thin-skinned contexts, in particular box folds, are able to accommodate only a finite amount of shortening (Ramsay, 1967; Ramsay and Huber, 1987). In addition, reverse slip along the fold-bounding faults or thrust planes locally thickened the brittle layer. Because the strength of a Mohr–Coulomb material increases with depth, hence thickness, fold growth and reverse faulting progressively hardened the structure, which eventually cancelled out the earlier weakening by strain softening. The folded and faulted cover thus became locally stronger than the thinner and undeformed adjacent area, which made it easier to form new folds in the undeformed blocks located in between the older structures, rather than continue to activate older folds. Only fault-related folds with a thick silicone layer at the base of the hanging-wall sequence could grow continuously, owing to the lower shear strength along their base. Eventually, no more new folds or thrusts formed and subsequent shortening was accommodated by growth of all existing structures (Fig. 9).

This overall propagation pattern markedly differs from the classic piggy-back or break-back propagation sequences described for fold-and-thrust belts above non-evaporitic detachments. As older folds were progressively abandoned during further shortening, new folds formed according to a back-and-forth, centripetal propagation sequence, which eventually resulted in closely-spaced, diachronous folds and thrusts affecting the entire width of the brittle layer.

4.2. Fold symmetry and asymmetry

The four models present different degrees of asymmetry. In the first two experiments (Models 1 and 2; Figs. 3A and B, 7 and 8), where the décollement layer covered the entire model (i.e. from moving endwall to fixed endwall) the folds were symmetrical and showed no systematic vergence. By contrast, in models having a deformable backstop and a foreland décollement pinch-out (Models 3 and 4; Figs. 3C and D, 5 and 6), there was, at least during the first stages of shortening, a definite preferential formation and/or growth

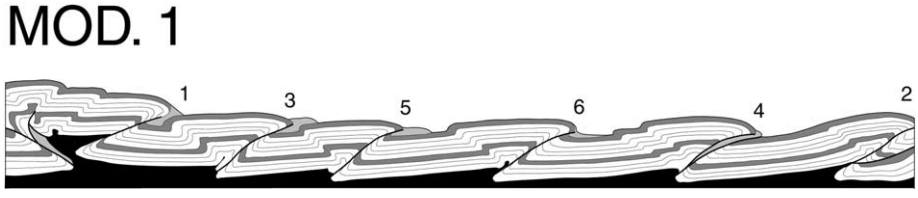

Fig. 8. Line drawing of a vertical cross-section in Model 1 (thin décollement, no deformable backstop and no décollement pinch-out). Shortening was accommodated by box folding. Box folding mechanism did not stretch fold hinges, hence no diapirs could pierce the cover. Symbols as in Fig. 5.

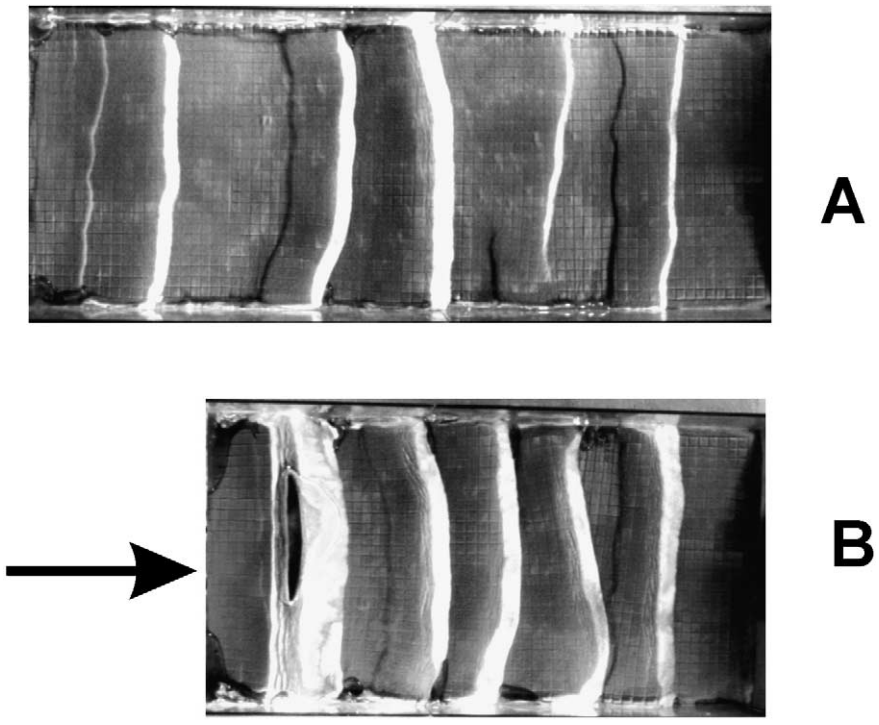

Fig. 9. Overhead photographs of Model 4 (deformable backstop and frontal décollement pinch-out) shot immediately after formation of the last structure (A) and at the end of the experiment (B). Comparison between A and B indicates that the last stage of shortening was accommodated by coeval tightening and growth of all structures in the model.

of forethrusts accompanied by tilting of the fault blocks toward the hinterland. In Model 3 (Fig. 5), where the décollement was thin, shortening was first accommodated along forethrusts and caused tilting of the fault blocks toward the hinterland. Later, block tilting ceased and transient backthrusts formed. In Model 4 (Fig. 6), where the décollement layer was thickest, only forethrusts formed and grew, except for very minor backthrusts (e.g. associated with Thrusts 1 and 2 in Fig. 6).

These observations suggest that the development of asymmetric structures was facilitated by the presence of both a deformable backstop in the hinterland and a foreland décollement pinch-out. Results also indicate that continued asymmetric growth requires the décollement layer to be sufficiently thick. Development of a preferred vergence and asymmetry of folds and thrusts has traditionally been attributed to high shear stresses at the base of the cover. In our models, however, the strength of the décollement was likely to be very low because its viscosity and the applied strain rate were low. For models with identical décollement viscosity and thickness and deformed under similar strain rates, only those having a deformable backstop and foreland pinch-out deformed asymmetrically.

The precise nature of the mechanical process that caused the asymmetry in Models 3 and 4 remains to be determined. In these models, the first two structures to form were asymmetric folds, one located on the hinterland side, near the deformable backstop, the other one located above the foreland pinch-out. In both locations, only forethrusts formed, presumably because basal friction there was high (décollement layer made of glass microbeads above the backstop, and no detachment beyond the pinch-out). Such an early development of asymmetric structures at both ends of the model may have influenced the state of stress within the rest of the cover underlain by the low-viscosity layer. Alternatively, the cause for subsequent asymmetric growth may be related to the tilting and distortion of the cover after early initiation of the hinterland and foreland forethrusts. On the hinterland side, the brittle cover forming the footwall of the thrust plane subsided below the regional datum, which also tilted the strata toward the hinterland. On the foreland side, the cover forming the hanging wall of the fault plane was raised above the regional datum and tilted toward the hinterland. It is possible that tilting of the cover associated with early slip along the two initial forethrusts may have triggered preferential formation of forethrusts in the rest of the model.

Whether asymmetric growth can persist throughout the entire deformation history is illustrated by the differences between Models 3 and 4. In Model 4, the thick décollement layer (initially 1 cm thick; Fig. 6) provided enough accommodation space for (1) the footwalls of each thrust plane to subside, and (2) the hanging walls to rise during the entire experiment. The bedding in the footwalls of the older thrusts rotated counterclockwise (i.e. toward the hinterland) by as much as 25°. In the cross-section in Fig. 6, the dip of the base of the rotated hanging-wall section was only within a few degrees to the orientation of the fault cutoff of the

underlying footwall block. The large amount of slip was made possible by the fact that the base of the hanging wall passively dragged up some source layer along the fault plane, further reducing the friction there.

In contrast, the initially thinner décollement provided less accommodation space in Model 3. Fig. 5 shows that, during the first stage of shortening, the fault blocks could subside, rise, or rotate, while shortening was accommodated solely by forethrusting up to the time of formation of Thrust 6 (Thrusts 1 to 6; Fig. 5). However, the fault blocks could no longer rotate or subside once the footwall was grounded onto the model's rigid base. Hence, secondary backthrusts formed, deformation became symmetrical, and the amount of finite rotation of the footwalls and hanging walls in Model 3 was lower (10° or less) than in Model 4.

The above factors, presence of deformable backstop, foreland décollement pinch-out, and thick décollement, also appear to have influenced the number of structures in the models. In Model 4, which had all three characteristics, shortening was accommodated by fewer structures, all long-lived forethrusts, because each structure could accommodate deformation by much more slip.

4.3. Diapirism

The differences shown by the models in diapir formation can also be related to the presence of a deformable backstop and the décollement thickness (Costa and Vendeville, 2001). Models 1 and 2, having no deformable backstop (Figs. 7 and 8), deformed by box folding of the brittle cover which was detached from its base along the entire model length. The underlying viscous layer thickened regionally but never rose diapirically because high horizontal compressive stresses prevented the source layer from piercing the strong roof section of the anticlines. By contrast, where there was a deformable backstop (Models 3 and 4), the innermost structure at the left part of the model was a fault-related fold (Figs. 5 and 6). A significant volume of viscous material was incorporated into the hanging wall, and was thus passively carried above the footwall. During further shortening, these fault-related folds continuously grew and their crests tightened, causing thinning of the brittle layer at the fold hinge and allowing the silicone to pierce and emerge.

The viscous layer flowed into the core of the fault-related folds until its footwall grounded, while diapirs rose until the source layer was depleted. Therefore, in Model 3, where the viscous layer was thinner, the footwall grounded early and the diapir at the core of the fold stopped rising before it could emerge (Fig. 5). In contrast, the footwall of the innermost fault-related fold grounded much later in Model 4, which initially had a thicker viscous layer. This allowed the silicone to flow throughout the entire deformation history. The diapir thus emerged at the surface and further deformed the fold forelimb (Fig. 6).

5. Some remarks on vertical movements and hydrocarbon maturation

All the characteristics of foldbelts detaching on salt described above imply that the presence of salt or evaporites can critically affect the thermal maturation and hydrocarbon migration pathways in fold-and-thrust belts. Thrusts are commonly assumed to propagate from the hinterland to the foreland according to a piggyback sequence. According to the burial history of such thrust-belts, hydrocarbons would first be generated at depth, then would migrate updip toward the basin's outer margin faster than the thrust front advances. In contrast, where foldbelts detach on salt, thrusts and anticlines can grow simultaneously while most of the synclines subside below the regional datum, which implies that structural hydrocarbon traps can form while the hydrocarbons are being generated. Furthermore, some amount of hydrocarbons may be trapped in the central part of the thrust belt rather than at the basin margins.

On the other hand, the high heat conductivity of rock salt also affects the hydrocarbon maturation. The highly conductive salt acts as a preferential pathway that channels heat to the surface. Salt domes, especially emergent salt domes, act as heat drains. This causes a regional cooling below salt masses that can affect the size, location and timing of the oil-generating window (Mello et al., 1995; Petersen and Lerche, 1996). The cooling effect caused by the presence of salt masses may be particularly important in fold-and-thrust belts. There, the heat drainage caused by salt may also act as a thermal compensator for the temperature increase associated with thrusting and footwall subsidence. The length of time during which oil may remain intact in the footwall sequence strongly depends on the thickness of the thrust sheet. However, our models suggest that the oil-generating window is larger and persists longer in fold-and-thrusts belts detaching above a thick evaporitic décollement. We used the geometry and kinematics observed on Model 2 (Figs. 3B and 7) to calculate the temperature decay using the approaches described by Mello et al. (1995) and Petersen and Lerche (1996). The temperature decay we found beneath the thrust sheet was 10–15% (corresponding to a temperature anomaly of about 20–30 °C) that represents an increase of about 10–15% (in both space and time) of the oil-generating window.

6. Conclusions

Our experiments demonstrate that the sequence of thrust propagation in fold-and-thrust belts detaching above a very weak viscous décollement is drastically different from that in belts detaching on stronger décollements. It is also different from that in models that were not insulated from lateral edge effects (e.g. Cotton and Koyi, 2000). Thrusts do not systematically propagate forward in a piggy-back fashion. Neither do they systematically propagate toward

the hinterland in break-back sequence. Instead, the frontal tip of the fold-and-thrust belt reaches the foreland pinch-out of the décollement early, which forces deformation to be accommodated by shortening the entire length of the system. New folds or thrusts form between older ones in a centripetal fashion and alternating between the foreland and the hinterland regions of the fold belt. There is no systematic thrust vergence or fold asymmetry where both the hinterland and foreland boundaries are vertical and rigid (Models 1 and 2; Figs. 7 and 8). By contrast, our results suggest that the presence of a deformable backstop and of a foreland salt pinch-out (Models 3 and 4; Figs. 5 and 6) favors preferential formation and growth of forethrusts, fold asymmetry, and tilting of the bedding toward the hinterland. However, asymmetric growth can subsequently cease if the source layer is too thin (Model 3; Fig. 5).

Our experiments also show that the formation of diapirs is strongly favored by the presence of a deformable backstop and thick viscous décollement. However, diapirism is restricted to the hanging wall of the fault-related fold in front of the backstop.

Our experimental results and their implications in terms of thermal history suggest that fold-and-thrust belts detaching on thick, weak viscous evaporites have distinct and specific structural and thermal patterns that greatly depart from the classic patterns of fold-and-thrust belts detaching on stronger detachments (e.g. shale).

References

Bellaiche, G., 1993. Sedimentary mechanisms and underlying tectonic structures of the northwestern Mediterranean margin, as revealed by comprehensive bathymetric and seismic surveys. Marine Geology 112 (1–4), 89–108.

Biot, M.A., 1961. Theory of folding of stratified viscoelastic media and its implication in tectonics and orogenesis. Geological Society of America Bulletin 72, 1595–1620.

Boyer, S.E., 1992. Geometric evidence for the synchronous thrusting in the south Alberta and northwest Montana thrust belts. In: McClay, K.R. (Ed.). Thrust Tectonics. Chapman & Hall, London, pp. 377–390.

Butler, R.W.H., Coward, M.P., Harwood, G.M., Knipe, R.J., 1987. Salt control on thrust geometry, structural style, and gravitational collapse along the Himalayan mountain front in the Salt Range of northern Pakistan. In: Lerche, I., O'Brien, J.J. (Eds.). Dynamical Geology of Salt and Related Structures. Academic Press, London, pp. 339–418.

Byerlee, J.D., 1978. Friction on rocks. Pure and Applied Geophysics 116, 615–626.

Camerlo, R.H., 1998. Geometric and kinematic evolution of detachment folds, Monterrey Salient, Sierra Madre Oriental, Mexico. Ms. Thesis, University of Texas at Austin, 399pp.

Cobbold, P.R., Rossello, E., Vendeville, B.C., 1989. Some experiments on interacting sedimentation and deformation above salt horizons. Bulletin de la Société Géologique de France, Série 8 5 (3), 453–460.

Costa, E., Vendeville, B.C., 2001. Diapirism in convergent settings triggered by hinterland pinch-out of viscous decollement: a hypothesis from modelling. In: Koyi, H.A., Mancktelow, N.S. (Eds.). Tectonic Modeling: A Volume in Honor of Hans Ramberg. Geological Society of America Memoir 193.

Cotton, J.T., Koyi, H.A., 2000. Modeling of thrust fronts above ductile and frictional detachments: application to structures in the Salt Range and Potwar Plateau, Pakistan. Geological Society of America Bulletin 112 (3), 351–368.

Coward, M.P., De Donatis, M., Mazzoli, S., Paltrinieri, W., Wezel, F.C., 1999. Frontal part of the northern Apennines fold and thrust belt in the Romagna-Marche area (Italy): shallow and deep structural styles. Tectonics 18, 559–574.

Dahlen, F.A., Suppe, J., Davis, D., 1984. Mechanics of fold-and-thrust belts and accretionary wedges: cohesive Coulomb theory. Journal of Geophysical Research 89, 10087–10101.

Davis, D.M., Engelder, T., 1985. The role of salt in fold and thrust belts. Tectonophysics 119, 67–88.

Davis, D.M., Engelder, T., 1987. Thin-skinned deformation over salt. In: Lerche, I., O'Brien, J.J. (Eds.). Dynamical Geology of Salt and Related Structures. Academic Press, London, pp. 301–337.

Davis, D.M., Lillie, R.J., 1994. Changing mechanical response during continental collision; active examples from the foreland thrust belts of Pakistan. Journal of Structural Geology 16 (1), 21–34.

Davis, D.M., Suppe, J., Dahlen, A., 1983. Mechanics of fold-and-thrust belts and accretionary wedges. Journal of Geophysical Research 88 (B2), 1153–1172.

Dixon, J.M., Liu, S., 1992. Centrifuge modelling of the propagation of thrust faults. In: McClay, K.R. (Ed.). Thrust Tectonics. Chapman & Hall, London, pp. 53–69.

Eisenstadt, G., Vendeville, B.C., Withjack, M.O., 1995. Introduction to Experimental Modeling of Tectonic Processes. Continuing Education Course Notes. Geological Society of America, unpaginated.

Fiduk, J.C., Weimer, P., Trudgill, B.D., Rowan, M.G., Gale, P.E., Phair, R.L., Korn, B.E., Roberts, G.R., Gafford, W.T., Lowe, R.S., Queffelec, T.A., 1999. The Perdido foldbelt, Northwest deep Gulf of Mexico. Part 2: seismic stratigraphy and petroleum systems. American Association of Petroleum Geologists Bulletin 83, 578–612.

Fischer, M.P., Jackson, P.B., 1999. Stratigraphic controls on deformation patterns in fault-related folds; a detachment fold example from the Sierra Madre Oriental, Northeast Mexico. Journal of Structural Geology 21 (6), 613–633.

Gaullier, V., Mart, Y., Bellaiche, G., Vendeville, B., Mascle, J., Zitter, T., The second leg "PRISMED II" scientific party, 2000. Salt tectonics in and around the Nile Deep-Sea Fan: insights from the "PRISMED II" cruise. In: Vendeville, B.C., Mart, Y., Vigneresse, J.L. (Eds.), Salt, Shale, and Igneous Diapirs in and around Europe. Geological Society of London Special Publication 174, pp. 111–129.

Hubbert, M.K., 1937. Theory of scale models as applied to the study of geologic structures. Geological Society of America Bulletin 48, 1459–1520.

Hubbert, M.K., Rubey, W., 1959. Role of fluid pressure in mechanics of over-thrust faulting: Parts I and II. Geological Society of America Bulletin 70, 115–205.

Kehle, R.O., 1970. Analysis of gravity sliding and orogenic translation. Geological Society of America Bulletin 81, 1641–1663.

Koyi, H., 1998. Modeling the role of gravity and lateral shortening in the Zagros mountain belt. American Association of Petroleum Geologists Bulletin 72, 1381–1394.

Krantz, R.W., 1991. Measurements of friction coefficients and cohesion for faulting and fault reactivation in laboratory models using sand and sand mixtures. Tectonophysics 188, 203–207.

Laubscher, H.P., 1977. Folds development in the Jura. Tectonophysics 37, 337–362.

Letouzey, J., Colletta, B., Vially, R., Chermette, J.C., 1995. Evolution of salt-related structures in compressional settings. In: Jackson, M.P.A., Roberts, D.G., Snelson, S. (Eds.), Salt Tectonics: A Global Perspective. American Association of Petroleum Geologists Memoir 65, pp. 41–60.

Liu Huiqi, McClay, K.R., Powell, D., 1992. Physical models of thrust wedges. In: McClay, K.R. (Ed.). Thrust Tectonics. Chapman & Hall, London, pp. 71–81.

Marrett, R.A., 1999. Stratigraphy and structure of the Jurassic and Cretaceous platform and basin systems of the Sierra Madre Oriental: a field book and related papers. South Texas Geological Society, 121 pp.

Marton, L.G., Tari, G.C., Lehmann, C.T., 2000. Evolution of the Angolan passive margin, West Africa, with emphasis on post-salt structural styles. In: Mohriak, W., Talwani, M. (Eds.), Atlantic Rifts and Continental Margins. American Geophysical Union Geophysical Monograph 115, pp. 129–149.

Mascle, J., Hugen, C., Benkhelil, M., Chamot-Rooke, N., Chaumillon, E., Foucher, J.P., Griboulard, R., Kopf, A., Lamarche, G., Volkonskaia, A., Woodside, J., Zitter, T., 1999. Images may show start of European–African plate collision. Eos, Transactions, American Geophysical Union 80 (37), 421–428.

McClay, K.R., 1989. Analogue models of inversion tectonics. In: Cooper, M.A., Williams, G.D. (Eds.), Inversion Tectonics. Geological Society [London] Special Publication 44, pp. 41–59.

Mello, U.T., Karner, G.D., Anderson, R.T., 1995. Role of salt in restraining the maturation of subsalt source rocks. Marine and Petroleum Geology 12, 697–716.

Peel, F.J., Travis, C.J., Hossack, J.R., 1995. Genetic structural provinces and salt tectonics of the Cenozoic offshore U.S. Gulf of Mexico: a preliminary analysis. In: Jackson, M.P.A., Roberts, D.G., Snelson, S. (Eds.), Salt Tectonics: A Global Perspective. American Association of Petroleum Geologists Memoir 65, pp. 109–151.

Petersen, K., Lerche, I., 1996. Temperature dependence of thermal anomalies near evolving salt structures: importance for reducing exploration risk. In: Alsop, G.I., Blundell, D.J., Davison, I. (Eds.), Salt Tectonics. Geological Society Special Publication 100, pp. 275–290.

Philippe, Y., Colletta, B., Deville, E., Mascle, A., 1996. The Jura fold-and-thrust belt: a kinematic model based on map-balancing. In: Ziegler, P.A., Horvàth, F. (Eds.), Peri-Tethys Memoir 2: Structure and Prospects of Alpine Basins and Forelands. Mémoires du Muséum d'Histoire Naturelle, Paris 170, pp. 235–261.

Price, R.A., Fermor, P.R., 1985. Structure section of the Cordilleran Foreland thrust and fold belt west of Calgary, Alberta. Paper—Geological Survey of Canada, 84-14.

Puigdefàbregas, C., Muñoz, J.A., Vergès, J., 1992. Thrusting and foreland basin evolution in the Southern Pyrenees. In: McClay, K.R. (Ed.). Thrust Tectonics. Chapman & Hall, London, pp. 247–254.

Ramberg, H., 1967. Gravity, Deformation and the Earth's Crust. Academic Press, London 214pp.

Ramsay, J.G., 1967. Folding and Fracturing of Rocks. McGraw-Hill, New York 568pp.

Ramsay, J.G., Huber, M.I., 1987. The Techniques of Modern Structural Geology. Academic Press, London, pp.1-700.

Rowan, M.G., 1997. 3-D geometry and evolution of a segmented detachment fold, Mississippi Fan fold belt, Gulf of Mexico. Journal of Structural Geology 19, 463–480.

Rowan, M.G., Peel, F.J., and Vendeville, B.C., in press. Gravity driven foldbelts on passive margins. In: K.R. McClay (Ed.), AAPG Memoir on Thrust Tectonics.

Sage, L., Letouzey, J., 1990. Convergence of the African and Eurasian Plate in the eastern Mediterranean. In: Letouzey, J. (Ed.), Petroleum and Tectonics in Mobile Belts. Proceedings of the IFP Exploration and Production Research Conference, Technips, Paris, pp. 49–68.

Schellart, W.P., 2000. Shear test results for cohesion and friction coefficients for different granular materials: scaling applications for their usage in analogue modelling. Tectonophysics 324, 1–16.

Spencer, J., Jeronimo, P., Tari, G., Vendeville, B., 1998. Protracted Salt Deformation History of the Lower Congo and Kwanza Basins of Offshore Angola. American Association of Petroleum Geologists Annual Convention Extended Abstracts 2, A629.

Stephanescu, M., Dicea, O., Tari, G., 2000. Influence of extension and compression on salt diapirism in its type area, east Carpathiam bend area, Romania. In: Vendeville, B.C., Mart, Y., Vigneresse, J.L. (Eds.), Salt, Shale and Igneous Diapirs in and around Europe. Geological Society of London Special Publication, pp. 131–147, in press.

Suppe, J., 1983. Geometry and kinematics of fault-bend folding. American Journal of Science 283, 684–721.

Trudgill, B.D., Rowan, M.G., Fiduk, J.C., Weimer, P., Gale, P.E., Korn, B.E., Phair, R.L., Gafford, W.T., Roberts, G.R., Dobbs, S.W., 1999. The Perdido foldbelt, Northwest deep Gulf of Mexico. Part 1: structural geometry, evolution and regional implications. American Association of Petroleum Geologists Bulletin 83, 88–113.

Valette, M., Benedicto, A., 1995. Chevauchements gravitaires halotectoniques dans le bassin distensif de Camargue (marge du golfe du Lion, SE de la France). Bulletin de la Societe Geologique de France, Huitieme Serie 166 (2), 137–147.

Vendeville, B.C., 1991. Thin-skinned compressional structures above frictional-plastic and viscous décollement layers. Geological Society of America, Abstract with Programs 23 (5), A423.

Vendeville, B.C., Cobbold, P.R., Davy, P., Brun, J.P., Choukroune, P., 1987. Physical models of extensional tectonics at various scales. In: Coward, M.P., Dewey, J.F., Hancock, P.L. (Eds.), Continental Extensional Tectonics, Geological Society of London Special Publication 28, pp. 95–107.

Von Huene, R., 1997. Mediterranean ridge structure; results from IMERSE. Eos, Transactions, American Geophysical Union 78 (15), 155.

Weijermars, R., Jackson, M.P.A., Vendeville, B.C., 1993. Rheological and tectonic modelling of salt provinces. Tectonophysics 217, 143–174.

Wu, S., 1993. Salt and slope tectonics offshore Louisiana. Ph.D. Dissertation, Rice University, Houston, Texas, 251pp.